

# Performance study and analysis method for a new-generation MIPAS experiment

Massimo Carlotti<sup>1,\*</sup> Elisa Castelli,<sup>2</sup> Bianca Maria Dinelli,<sup>2</sup> and Enzo Papandrea<sup>1</sup>

<sup>1</sup>Dipartimento di Chimica Industriale, University of Bologna, Viale Risorgimento 4, 40136 Bologna, Italy

<sup>2</sup>ISAC-CNR, Via P. Gobetti 101, 40129 Bologna, Italy

\*Massimo.carlotti@unibo.it

**Abstract:** This study fits within the ongoing activities aimed at filling the lack of an operational IR limb sounder after the ENVISAT fault. Notably, we report the performance of a possible evolution of the MIPAS experiment. The strategy proposed for the new experiment (that we denote as MIPAS2k) is derived from the PREMIER infrared limb sounder (IRLS) and relies on both 1D array detector technology and reduction of the spectral resolution to achieve dense atmospheric sampling. We define observation parameters and report, as an example, the performance obtained by MIPAS2k when measuring O<sub>3</sub> fields. The information load (IL) analysis was exploited to assess the sensitivity of MIPAS2k and to select optimal spectral intervals for retrieval tests on simulated observations of the new experiment. The results of the IL analysis suggest a new approach to the retrieval strategy (denoted as *full-2D*) in which the unknown parameter is no longer an element of the altitude profile but the constant value taken by the atmospheric quantity within a parcel (denoted as “clove”) of the 2D discretization. We demonstrate that the clove homogeneity assumption generates errors that are below the spectral noise of MIPAS2k when an appropriate clove thickness is used. *Full-2D* retrievals have been carried out on MIPAS2k simulated observations corresponding to a high resolution model atmosphere. We report a test case on O<sub>3</sub> VMR in which the retrieval precision is better than 5% between 20 and 40 km and better than 30% in the upper troposphere-lower stratosphere. We test the ability of MIPAS2k to reconstruct a fine O<sub>3</sub> structure present in the model atmosphere and we show how this structure would have been represented by MIPAS when measuring the same scenario. We have estimated the spatial resolution of MIPAS2k products by means of the perturbation approach that, in simulated retrievals, can be adopted to evaluate the averaging kernel of the retrieval parameters. For O<sub>3</sub> we have found the estimates of 200 km and 2.5 km for the horizontal and vertical resolutions respectively.

©2014 Optical Society of America

**OCIS codes:** (150.1135) Algorithms; (010.1280) Atmospheric composition; (280.4991) Passive remote sensing; (100.3190) Inverse problems; (000.3860) Mathematical methods in physics.

---

## References and links

1. European Space Agency, ed., “ENVISAT-MIPAS: an instrument for atmospheric chemistry and climate research,” ESA Rep. SP-1229. (European Space Research and Technology Center, Noordwijk, The Netherlands, March 2000).
2. P. Raspollini, F. Barbara, B. Carli, M. Carlotti, E. Castelli, S. Ceccherini, A. Dehn, M. De Laurentis, B. M. Dinelli, A. Dudhia, T. Fehr, H. Fischer, J.-M. Flaud, B. Funke, M. Hoepfner, M. Kiefer, M. Lopez-Puertas, H. Oelhaf, F. Niro, J. J. Remedios, M. Ridolfi, H. Sembhi, L. Sgheri, T. von Clarmann, and H. Weber, “Ten years of MIPAS measurements with ESA Level 2 processor V6,” in Proceedings of Advances in Atmospheric Science and Applications (ATMOS 2012) Bruges, 18–22 Jun, 2012.
3. P. Raspollini, B. Carli, M. Carlotti, S. Ceccherini, A. Dehn, B. M. Dinelli, A. Dudhia, J.-M. Flaud, M. López-Puertas, F. Niro, J. J. Remedios, M. Ridolfi, H. Sembhi, L. Sgheri, and T. von Clarmann, “Ten years of MIPAS

- measurements with ESA Level 2 processor V6 - Part 1: Retrieval algorithm and diagnostics of the products,” *Atmos. Meas. Tech.* **6**(9), 2419–2439 (2013).
4. ESA, Candidate Earth Explorer Core Missions – Report for Assessment: PREMIER – PROcess Exploitation through Measurements of Infrared and millimetre-wave Emitted Radiation, SP-1313/5, ESA Publications Division, ESTEC, Keplerlaan 1, 2200 AG Noordwijk, The Netherlands, (2008).
  5. M. Carlotti, “Global-fit approach to the analysis of limb-scanning atmospheric measurements,” *Appl. Opt.* **27**(15), 3250–3254 (1988).
  6. M. Ridolfi, B. Carli, M. Carlotti, T. von Clarmann, B. M. Dinelli, A. Dudhia, J. M. Flaud, M. Höpfner, P. E. Morris, P. Raspollini, G. Stiller, and R. J. Wells, “Optimized forward model and retrieval scheme for MIPAS near-real-time data processing,” *Appl. Opt.* **39**(8), 1323–1340 (2000).
  7. M. Carlotti and B. Carli, “Approach to the Design and Data Analysis of a Limb-Scanning Experiment,” *Appl. Opt.* **33**(15), 3237–3249 (1994).
  8. M. Carlotti, B. M. Dinelli, P. Raspollini, and M. Ridolfi, “Geo-fit approach to the analysis of limb-scanning satellite measurements,” *Appl. Opt.* **40**(12), 1872–1885 (2001).
  9. M. Carlotti and L. Magnani, “Two-dimensional sensitivity analysis of MIPAS observations,” *Opt. Express* **17**(7), 5340–5357 (2009).
  10. M. Carlotti, E. Castelli, and E. Papandrea, “Two-dimensional performance of MIPAS observation modes in the upper troposphere/lower-stratosphere,” *Atmos. Meas. Tech.* **4**(2), 355–365 (2011).
  11. H. Fischer, M. Birk, C. Blom, B. Carli, M. Carlotti, T. von Clarmann, L. Delbouille, A. Dudhia, D. Ehalt, M. Endemann, J.-M. Flaud, R. Gessner, A. Kleinert, R. Koopman, J. Langen, M. L’opez-Puertas, P. Mosner, H. Nett, H. Oelhaf, G. Perron, J. J. Remedios, M. Ridolfi, G. Stiller, and R. Zander, “MIPAS: an instrument for atmospheric and climate research,” *Atmos. Chem. Phys.* **8**(8), 2151–2188 (2008), doi:10.5194/acp-8-2151-2008.
  12. M. Carlotti, G. Brizzi, E. Papandrea, M. Prevedelli, M. Ridolfi, B. M. Dinelli, and L. Magnani, “GMTR: two-dimensional geo-fit multitarget retrieval model for michelson interferometer for passive atmospheric sounding/environmental satellite observations,” *Appl. Opt.* **45**(4), 716–727 (2006).
  13. B. M. Dinelli, E. Arnone, G. Brizzi, M. Carlotti, E. Castelli, L. Magnani, E. Papandrea, M. Prevedelli, and M. Ridolfi, “The MIPAS2D database of MIPAS/ENVISAT measurements retrieved with a multi-target 2-dimensional tomographic approach,” *Atmos. Meas. Tech.* **3**(2), 355–374 (2010).
  14. M. Kiefer, E. Arnone, A. Dudhia, M. Carlotti, E. Castelli, T. von Clarmann, B. M. Dinelli, A. Kleinert, A. Linden, M. Milz, E. Papandrea, and G. Stiller, “Impact of temperature field inhomogeneities on the retrieval of atmospheric species from MIPAS IR limb emission spectra,” *Atmos. Meas. Tech.* **3**(5), 1487–1507 (2010).
  15. M. Ridolfi, L. Magnani, M. Carlotti, and B. M. Dinelli, “MIPAS-ENVISAT limb-sounding measurements: trade-off study for improvement of horizontal resolution,” *Appl. Opt.* **43**(31), 5814–5824 (2004).
  16. A. Dudhia, V. L. Jay, and C. D. Rodgers, “Microwindow selection for high-spectral-resolution sounders,” *Appl. Opt.* **41**(18), 3665–3673 (2002).
  17. M. Carlotti, E. Arnone, E. Castelli, B. M. Dinelli, and E. Papandrea, “Position error in profiles retrieved from MIPAS observations with a 1-D algorithm,” *Atmos. Meas. Tech.* **6**(2), 419–429 (2013).
  18. A. Dudhia, University of Oxford, AOPP, Oxford, UK, (personal communication, 2013).
  19. J. T. Houghton, *The Physics of Atmospheres*, 2nd ed. (Cambridge University, 1977).
  20. J. J. Remedios, R. J. Leigh, A. M. Waterfall, D. P. Moore, H. Sembhi, I. Parkes, J. Greenhough, M. P. Chipperfield, and D. Hauglustaine, “MIPAS reference atmospheres and comparisons to V4.61/V4.62 MIPAS level 2 geophysical data sets,” *Atmos. Chem. Phys. Discuss.* **7**(4), 9973–10017 (2007).
  21. M. Carlotti, B. M. Dinelli, E. Papandrea, and M. Ridolfi, “Assessment of the horizontal resolution of retrieval products derived from MIPAS observations,” *Opt. Express* **15**(16), 10458–10472 (2007).
  22. T. von Clarmann, M. Hoepfner, S. Kellmann, A. Linden, S. Chauhan, B. Funke, U. Grabowski, N. Glatthor, M. Kiefer, T. Schieferdecker, G. T. Stiller, and S. Versick, “Retrieval of temperature, H<sub>2</sub>O, O<sub>3</sub>, HNO<sub>3</sub>, CH<sub>4</sub>, N<sub>2</sub>O, ClONO<sub>2</sub> and ClO from MIPAS reduced resolution nominal mode limb emission measurements,” *Atmos. Meas. Tech.* **2**, 159–175 (2009).

## 1. Introduction

The Michelson Interferometer for Passive Atmospheric Sounding (MIPAS) has operated on board the ENVISAT satellite from July 2002 to April 2012 when the spacecraft ceased communications. Except for an interruption lasting about six months, MIPAS has measured the Earth’s atmosphere throughout the ENVISAT lifetime. In this operational period the analysis of MIPAS spectra daily provided about 1000 altitude profiles of key atmospheric constituents as well as of pressure and temperature. This huge amount of data gave origin to a wide scientific production. MIPAS was very successful but was conceived more than twenty years ago [1]; in this time lapse new technologies have evolved and lessons have been learnt from the analysis of about ten years of measurements [2,3].

The loss of ENVISAT caused a breakdown in the monitoring of important geophysical parameters that can be acquired by limb sounders measuring the atmospheric emission. The

PREMIER experiment [4] was proposed to restore the data flow with improved performance but it was not selected as payload on the forthcoming Earth Explorer 7 platform.

A major property of the retrieved atmospheric quantities is their spatial resolution: in this respect the MIPAS observation strategies were the result of a trade-off between spectral resolution and density of the atmospheric sampling. The global fit [5], adopted by MIPAS ground segment for the routine analyses [6] as well as other one-dimensional (1D) retrieval algorithms, made possible to assess, in the vertical domain, the complex interdependence between atmospheric sampling, retrieval grid, and properties of the retrieval products such as precision and vertical resolution [7]. In the horizontal domain the atmospheric sampling of a MIPAS-like instrument is limited by the time spent by the moving mirrors to reach the maximum optical path difference (that defines the spectral resolution) combined with the satellite motion. A realistic assessment of this trade-off was attained through the evolution of the data analysis and was further tested when the spectral resolution of MIPAS had to be reduced to deal with a problem in the mirror slides (see Sect. 2). The advent of the two-dimensional (2D) analysis approach [8] gave a new perspective to the horizontal atmospheric sampling and added this element to the interdependence system by including horizontal retrieval grid and horizontal resolution. Afterwards, the information load (IL) analysis [9] made possible the visual representation of the actual 2D atmospheric sampling then enabling the comparison of the performance of different observation strategies [10].

In this paper we exploit the characterization of MIPAS measurements, achieved along the full mission, to design observational parameters and a retrieval strategy for a hypothetical new-generation MIPAS-like experiment for which the geometrical atmospheric sampling is enhanced by exploiting the array detector technology in conjunction with reduced spectral resolution. The envisaged experiment (that we denote as MIPAS2k) is focalized to measure the upper troposphere-lower stratosphere (UTLS) and is a simplified version of the infrared limb sounder (IRLS), one of the two instruments of PREMIER. The scientific background and the expected impact of this kind of measurements can be found in Ref. [4] and references therein. The concept of MIPAS2k is less ambitious with respect to IRLS because it does not consider measurements outside the orbit plane, however it is meant to measure the status of stratosphere and upper troposphere with precision and spatial resolutions that could not be achieved when MIPAS was designed.

Features of the MIPAS experiment that are relevant for our study are briefly summarized in Sect. 2 together with the rationale of the 2D tools expressly developed for MIPAS and exploited in the present study. In order to define an observational strategy for the hypothetical experiment we highlight, in Sect. 3, the indications that emerge from the IL analysis of MIPAS observations. From this starting point we formulate, in Sect. 4, hypotheses for observational parameters of MIPAS2k and we select spectral intervals that, in compliance with the observational strategy, are suitable for the retrieval of MIPAS2k targets. In Sect. 4 we also compare the IL analysis of the selected MIPAS2k observations with that of some MIPAS observation modes. In Sect. 5 we introduce a new approach to the 2D retrieval strategy that is consistent with the IL analysis. In Sect. 6 we assess the performance of MIPAS2k retrieval products and we compare the capability of MIPAS and MIPAS2k to reproduce, with simulated retrievals, a fine atmospheric structure. In Sect. 7 we assess the spatial resolution of the new experiment. Computational details are provided in Sect. 8 and conclusions are drawn in Sect. 9. In this paper we report the performance of MIPAS2k when measuring  $O_3$  fields as representative of the results obtained for the other considered targets:  $H_2O$ ,  $HNO_3$ ,  $CH_4$ ,  $N_2O$ . Actually,  $O_3$  is a meaningful case study because of its abundance and non-monotonic vertical distribution.

## 2. The MIPAS experiment

MIPAS measured the infra-red atmospheric emission (from a nearly polar orbit) with consecutive backward-looking limb-scans having the line of sight lying near the orbit plane.

An exhaustive description of the experiment can be found in [11]. MIPAS operational life can be divided into two parts: the Full Resolution (FR) mission when the instrument was operated at the spectral resolution of  $0.035\text{ cm}^{-1}$  unapodised, and the Optimised Resolution (OR) mission when spectral resolution was degraded to  $0.0625\text{ cm}^{-1}$  because of a problem with the interferometric slides. Most of MIPAS measurements were carried out in the “nominal” observation mode (NOM) where each limb-scan had 17 and 27 observation geometries in the FR and OR mission respectively. In the OR mission the 11 lowest tangent altitudes of the NOM observation mode are separated by 1.5 km; the separation increases to 2, 3, and 4 km in the next groups of 5, 5, and 6 tangent altitudes respectively. This vertical sampling generates 96 limb-scans per orbit separated by about 410 km. The lowest altitude of the limb-scan is latitude dependent in order to imitate the tropopause behaviour. MIPAS was also operated in several “special” observation modes; details are provided for those used in the next section. In the FR mission a special mode denoted as S6 (used for only 12 orbits in July 2003) was designed to sound the UTLS region with a fine geometrical sampling. With S6 the horizontal atmospheric sampling of about 120 km was achieved by degrading the spectral resolution to  $0.1\text{ cm}^{-1}$  and by concentrating 12 observation geometries at tangent altitudes in the UTLS. In the OR mission two special observation modes (denoted as UTLS-1 and UTLS-2) were also designed to sound the UTLS. In this case the finer atmospheric sampling was accomplished by using a reduced number of observation geometries per limb-scan concentrated in the UTLS. The best horizontal sampling (180 km) was achieved by UTLS-2 that, however, was operated for only 35 orbits. Actually, when planning the OR mission the horizontal sampling was believed of minor importance because 1D retrieval algorithms were used to produce level 2 data and priority was given to the vertical resolution of the products. The 1.5 km vertical sampling, provided by the nominal mode in the UTLS, was then considered satisfactory.

Later on, the 2D Geo-fit analysis method [8] was proposed and implemented in the operational code GMTR (Geo-fit Multi Target Retrieval) [12] for routine analysis of MIPAS observations. In this method the 2D retrieval grid is fully independent from the measurement grid and is used to model the horizontal structures of the atmosphere. Therefore the separation (both vertical and horizontal) between retrieval grid points can be chosen on the basis of only the trade-off between precision and spatial resolution. The MIPAS2D database [13] was generated with the GMTR analysis system; it was proven that MIPAS2D products do not suffer by the errors due to neglecting the horizontal structures of the atmosphere, typical of the 1D algorithms [14]. GMTR made possible the evaluation of the horizontal resolution of MIPAS products and the study of the trade-off between the horizontal spacing of the retrieval products and the retrieval error affecting them [15]. The 2D system highlighted some weakness of the MIPAS observation strategies and to identify improvements that could be adopted to avoid them.

Irrespective of the used retrieval algorithm, the analysis of MIPAS observations is carried out on a selected number of narrow (less than  $3\text{ cm}^{-1}$  wide) spectral intervals, called microwindows (MWs), which carry optimal information on the target quantity [16].

### 3. Information Load of MIPAS observations

#### *Background*

The IL analysis was introduced to study the sensitivity of MIPAS observations to geophysical targets in the frame of a 2D retrieval approach [9]. In the present study we have exploited the IL performance of different MIPAS observation modes to identify the observation strategy for a new experiment, and to assess the improvements that can be achieved in the sensitivity of the observations. We recall here the basic concepts of the IL analysis that are also used as a base in the strategy of the new retrieval approach proposed in Sect. 5 for MIPAS2k.

For the Geo-fit analysis of limb-scanning observations the atmosphere is partitioned on both the vertical and the horizontal domains by means of consecutive altitude levels and

vertical radii [8]. This discretization leads to a web-like picture in which the point defined by the crossing of a level with a radius is denoted as “node” and the plane figure delimited by consecutive levels and radii is denoted as “clove”. The typical width of the cloves in operational MIPAS retrievals is 1 latitude deg (~110 km); the clove thickness strongly depends on altitude and ranges from 0.5 to 3 km. Figure 1 shows (with highly distorted scale) an example of the 2D discretization with one clove highlighted in green. In the MIPAS observation strategy, backward looking limb-scans are continuously repeated along the orbit track. It follows that, as illustrated in Fig. 1, the Line Of Sight (LOS) of several observation geometries may cross a given clove of the atmospheric discretization.

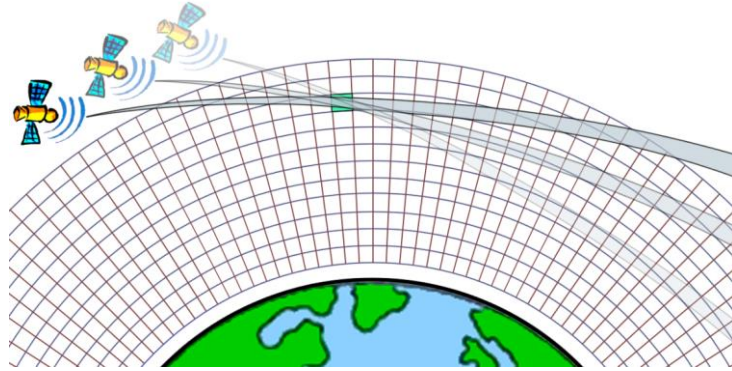


Fig. 1. 2D discretization of the atmosphere. A clove, highlighted in green, is crossed by the LOS of three observation geometries.

If the simultaneous analysis of all the observation geometries is considered (as in the case of Geo-fit), we can assign to clove  $h$  the *information load* scalar quantifier ( $\Omega$ ) with respect to the geophysical parameter  $q$ .  $\Omega$  is defined in Eq. (7) of Ref. [9], and can be written as:

$$\Omega(q, h) = [(\mathbf{k}^T \mathbf{k})_h]^{1/2} \quad (1)$$

where  $\mathbf{k}$  is a vector containing the derivatives, with respect to  $q$ , of all the observations that depend on the value of  $q$  in clove  $h$ .

If the observations are affected by different spectral noise levels (as, e.g., are in different MIPAS spectral bands) it is more appropriate to use the weighted information load ( $W\Omega$ ) defined as:

$$W\Omega(q, h) = [(\mathbf{k}^T \mathbf{S}^{-1} \mathbf{k})_h]^{1/2} \quad (2)$$

where  $\mathbf{S}$  is the variance-covariance matrix of the observations relative to all the spectral points that contribute to the information load of clove  $h$  [17].

In the hypothetical retrieval of the target quantity  $q$  in clove  $h$  the random error on the retrieved value of  $q$  is connected with the quantity  $1/W\Omega$  (see Ref. [9]).

A map of the  $W\Omega$  quantifier, calculated for each clove of the 2D atmospheric discretization (see examples below), enables evaluation of the 2D distribution of  $W\Omega$  with respect to the geophysical parameter  $q$ . In these maps:

- The values of  $W\Omega$  measure the amount of information contained in the corresponding cloves; the precision of the retrieval products is therefore connected with these values [9,17].
- The spatial distribution of  $W\Omega$  indicates the regions of the atmosphere where the information is gathered from, when operating a retrieval analysis.

It follows that the IL analysis provides a tool to compare the performance of different observation strategies and/or of different sets of spectral intervals when they are used in retrieval analyses. The  $W\Omega$  maps also indicate the optimal strategy to select altitudes and latitudes of the retrieval grid.

#### *Analysis of MIPAS observation modes*

The left panel of Fig. 2 shows a map of the  $W\Omega$  distribution with respect to  $O_3$  VMR, calculated with the observational parameters of orbit 30958 (January 31, 2008) when MIPAS was operated in OR NOM observation mode (see Sect. 2). In this panel values of  $W\Omega$  are

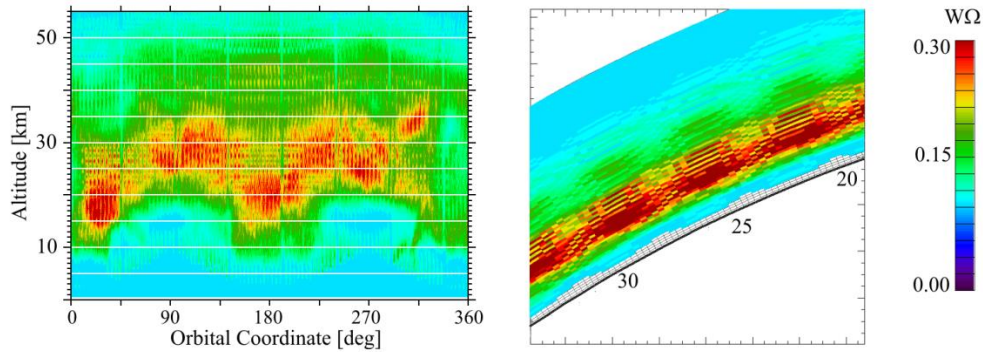


Fig. 2. Left panel: Ozone  $W\Omega$  distribution for an orbit of the OR nominal MIPAS observation mode. Horizontal lines mark altitudes from 5 to 50 km at 5 km steps. Right panel: detail of the  $W\Omega$  distribution (in polar coordinates) around the OC value of 25 deg. The atmosphere is expanded by a factor of 10 with respect to the Earth's radius.

reported as a function of altitude and of the orbital coordinate (OC; the polar coordinate originating at North Pole and spanning the orbit plane in the counter-clockwise direction). The right panel of Fig. 2 shows a detail of the  $W\Omega$  distribution around the OC value of 25 deg; here the orbital coordinate is reported in its geographical layout, with polar coordinates, and the atmosphere is expanded by a factor of 10 with respect to the Earth's radius. Maps of Fig. 2 are generated by the set of (five) MWs analyzed by the MIPAS ground segment to retrieve the  $O_3$  VMR profiles. The 2D  $O_3$  distribution used for these calculations (as well as for all the other tests reported in this paper) has been derived from the ECMWF (European Centre for Medium-Range Weather Forecasts) atmospheric fields along the considered orbit (the horizontal separation between altitude profiles that define these ECMWF fields is 1.125 deg). In the case of VMR targets (as it is  $O_3$  shown in Fig. 2) the derivatives in vector  $\mathbf{k}$  (Eqs (1) and (2)) are calculated with respect to the logarithm of VMR; the resulting  $W\Omega$  values are then correlated with the relative error of the target quantity [7].

In the right-hand panel of Fig. 2 we can appreciate vertical discontinuities in the  $W\Omega$  intensity: they are due to the discretization adopted in modelling the instrument Field Of View (FOV) ( $\sim 3$  km at tangent points) rather than to the geometrical sampling of the atmosphere. In the left-hand panel of Fig. 2 gaps of  $W\Omega$  intensity can be observed in the 5–10 km altitude range that extend upward while approaching the equator. They are due to the observation strategy used in the NOM mode of the OR mission (see Sect. 2) where a latitude-dependent limb-scanning pattern imitates the latitudinal tropopause fluctuation. Figure 2 also shows that the MIPAS geometrical sampling of the atmosphere generates horizontal discontinuities. Uniform  $W\Omega$  distributions are desirable because they allow evenly spaced horizontal retrieval grids where the constant separation among the retrieved profiles can be chosen on the basis of only the trade-off between their spatial resolution and precision [15].

On the other hand, the  $W\Omega$  horizontal discontinuities make the assessment of horizontal resolution difficult [17].

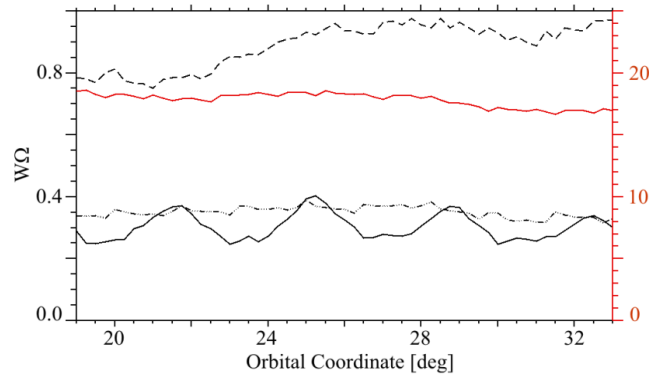


Fig. 3. Sample distributions of the  $O_3$   $W\Omega$  quantifier at 20 km in the 19-33 deg OC interval. Black lines, measured by the left-hand y axis, refer to different MIPAS observation modes: solid to OR NOM, dot-dashed and dashed to UTLS-2 and S6 respectively. The red line, measured by the right-hand y axis, refers to MIPAS2k.

The analysis of the different observation modes used during the MIPAS lifetime led to understand the behaviour of the horizontal  $W\Omega$  distribution as a function of the horizontal sampling. Figure 3 shows plots of  $W\Omega$  at 20 km altitude for different observation strategies. In this figure the OC interval is the same as in the right panel of Fig. 2. The black lines of Fig. 3 refer to different MIPAS observation modes (see Sect. 2) and are measured by the left-hand y axis: the solid line refers to the OR NOM mode (shown in Fig. 2) while the dot-dashed and dashed lines refer to UTLS-2 and S6 modes respectively. Looking at Fig. 3 it is possible to assess how, in a 2D context, the amount of information available for the retrieval analysis increases while increasing the geometrical atmospheric sampling. Furthermore, as expected, a finer atmospheric sampling induces homogeneity in the horizontal information distribution. The red line of Fig. 3, measured by the right-hand y axis, will be discussed in Sect. 4.

The IL analysis of MIPAS observation modes indicates that the observation strategy of a successor experiment, should act on atmospheric sampling to generate strong and uniform  $W\Omega$  fields in order to get high performance of the retrieval products.

#### 4. Observational parameters and MWs selection for MIPAS2k

Several studies led to define the observational strategies of the IRLS/PREMIER experiment [4] both prior to the proposal and during the ESA (European Space Agency) selection process. The *chemistry mode* of IRLS exploits a set of observational parameters that we have adopted for MIPAS2k because they are consistent with the indications provided by the IL analyses of the MIPAS observation modes. These criteria were also the starting point for the selection of spectral intervals suitable for retrieval tests (see Sect. 6).

The IRLS experiment was conceived to operate with a 2D array detector capable of simultaneously measure a set of backward-looking limb-scans along and sideways with respect to the orbit plane. This feature should have enabled IRLS to determine 3D fields of target geophysical quantities. The less ambitious hypothesis that we envisage for MIPAS2k is a 1D array detector that, as MIPAS, measures consecutive backward-looking limb-scans just in the orbit plane but a single stroke of the interferometric mirrors is sufficient to acquire a whole limb-scan. This strategy, combined with the spectral resolution of  $0.2 \text{ cm}^{-1}$  makes the separation between consecutive limb-scans of about 100 km leading to 400 limb-scans per orbit. The spectral range envisaged for MIPAS2k roughly corresponds to the overall coverage of MIPAS bands A, AB, and B [11]. Table 1 reports the main observational parameters of MIPAS2k. Minor instrumental and observational parameters (not reported in Table 1) have

been maintained as for MIPAS. The carrying platform has been assumed in the same orbit of ENVISAT (polar at altitude ~790 km, period of 100.6 min).

**Table 1. Observational Parameters of MIPAS2k**

Along track sampling (km)	100
Limb-scanning step (km)	2
Altitude range (km)	6 - 54
Spectral range ( $\text{cm}^{-1}$ )	685 - 1650
Spectral resolution ( $\text{cm}^{-1}$ )	0.2
Noise level rms ( $\text{nW/cm}^2 \text{ sr cm}^{-1}$ )	1.0
Vertical instantaneous FOV (km)	2.2

In order to define optimal spectral intervals to be analyzed for the retrieval of the  $\text{O}_3$  VMR, we started from a set of 5 MWs that were selected for the IRLS instrument [18]. The  $W\Omega$  distribution of each MW was then analyzed in order to sort out the MWs that provide the best compromise between  $W\Omega$  intensity and altitude coverage in the UTLS region [17]. In this process, a threshold was imposed to the number of spectral points in order to limit the demand of computer resources (see Sect. 8). With these criteria the final choice was for two MWs identified by the spectral intervals:  $721.2 - 724.2 \text{ cm}^{-1}$  and  $770.8 - 773.6 \text{ cm}^{-1}$ .

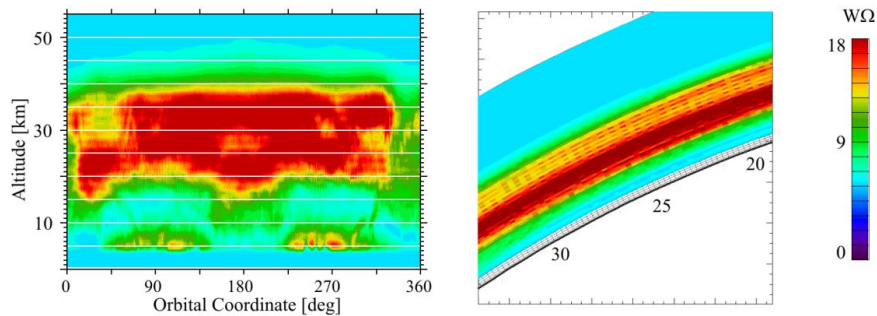


Fig. 4. Maps of  $W\Omega$  w.r.t.  $\text{O}_3$  VMR for an orbit of MIPAS2k. Plotting formats are as in Fig. 2.

Figure 4 shows the map of the  $W\Omega$  distribution with respect to  $\text{O}_3$  VMR calculated using the observational parameters of Table 1 and the two MWs selected for MIPAS2k. The format of this figure is the same as in Fig. 2 except for the colour scale that, in Fig. 4, is enhanced by a factor of 60. The comparison of Figs 2 and 4 highlights the dramatic increase in  $W\Omega$  intensity that is obtained with MIPAS2k observations even if only two MWs are used. A quantitative evaluation of this increase is provided by the red line of Fig. 3 (measured by the right-hand y axis) that refers to the  $W\Omega$  quantifier at 20 km for MIPAS2k observations.

The intensity increases by a factor of about 50 with respect to MIPAS NOM and UTLS-2 observations and by a factor of about 20 with respect to MIPAS S6 observations. Beside the improvements obtained for the  $W\Omega$  intensity, we notice that oscillations do not appear in the red curve of Fig. 3.

The comparative results of the IL analyses are expected to reflect into an overall better performance of MIPAS2k with respect to MIPAS measurements. Before showing the quality of the MIPAS2k retrieval products we introduce, in the next section, the new retrieval approach that we have exploited for the analysis of MIPAS2k observations.

## 5. The full-2D retrieval approach

The Geo-fit 2D algorithm [8], designed for MIPAS observations, retrieves altitude distribution profiles at geo-located positions just as most of the 1D algorithms do. The radiative transfer calculations within the Geo-fit analysis require defining the value of the atmospheric quantities on each node of the 2D fine grid (see Sect. 3). This is achieved by



interpolating the closest vertical profiles of the atmospheric quantities on each node. The high and uniform W $\Omega$  values verified for MIPAS2k (see Sect. 4) suggest unprecedented quality of the retrieval products in terms of both precision and spatial resolution (that is the goal of our study). As a consequence, the vertical and horizontal dimension of the clove is expected to be comparable with the local spatial resolutions. These considerations suggest a different approach to the retrieval strategy: the generic retrieval parameter is no longer defined as the element of an altitude profile but as the constant value of the geophysical quantity within a clove of the 2D discretization. This approach avoids the interpolations used in the Geo-fit and is consistent with the IL analysis.

The new retrieval strategy, that we denote as *full-2D*, implies homogeneity of the atmosphere within each clove. This assumption is justified if the dimension of the clove is infinitesimal or small enough to provide an acceptable approximation of this condition. Moreover, the demand of computer resources is strongly affected by the clove dimensions because they determine the total number of cloves and therefore, in the *full-2D* approach, the number of the parameters to be retrieved. For these reasons compromise values need to be assessed for the size of cloves by evaluating their trade-off with the quality of the retrieval products. From the point of view of the retrieval system, the homogeneity assumption changes the radiative properties of a clove mainly through the values of temperature (T) and pressure (P) that are assigned to it. In the case of Geo-fit, *effective* values of T and P are determined by using the Curtis-Godson integrals [19] that (calculated by interpolating between the values at the four nodes) account for the atmospheric variability along the optical path within the clove. In the case of *full-2D* the effective values are substituted by average values of each atmospheric quantity within the clove. In order to evaluate the impact of this approximation we have simulated spectra using different 2D discretizations of the atmosphere with clove dimensions ranging from 0.25 to 2 deg in width (about 30 to 220 km), and from 0.25 to 2 km in thickness. Since the vertical gradients are, in general, much stronger than the horizontal ones, the vertical dimension of the cloves is more critical. In Fig. 5 we show the difference between spectra calculated with the *full-2D* and with the Geo-fit approach over the lower part of a mid-latitude limb scan. The red line of this figure refers to simulations operated, on the two O<sub>3</sub> MWs with clove dimensions of 1 deg as width and 2 km as thickness. Differences are relative to all the spectral points of the two MWs. In Fig. 5 the MWs are paired and lined up along the x axis that reports the corresponding tangent altitudes. The blue horizontal lines represent the r.m.s. of the spectral noise (see Table 1). The red line of Fig. 5 shows that, with the adopted discretization, the clove homogeneity assumption introduces distortions that exceed the noise especially below 22 km. In the upper part of the limb scan (not shown) differences do not exceed the noise level. The green and blue lines of Fig. 5 show the spectral differences in the case of 1 km and 0.5 km as clove thickness respectively.

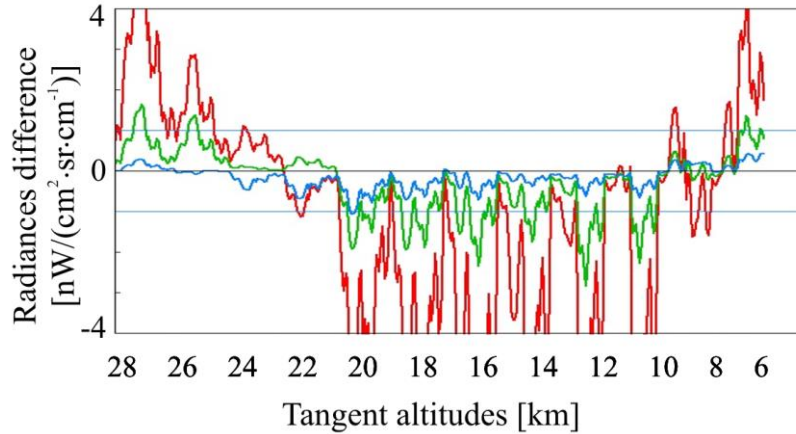


Fig. 5. Differences between *full-2D* and Geo-fit simulations calculated for all the spectral points of the two O<sub>3</sub> MWs over the lower part of a mid-latitude limb scan. The two MWs are paired and lined up along the *x* axis that reports the corresponding tangent altitudes. Red line: simulations with cloves that are 2 km thick and 1 deg wide. Green and blue lines: simulations with clove thickness of 1.0, and 0.5 km respectively. The horizontal blue lines delimit the r.m.s. of MIPAS2k spectral noise.

In Fig. 5 we can see that, as expected, the amplitude of the differences decreases with reducing the clove thickness and stays below the spectral noise when the cloves are 0.5 km thick. The same strategy, applied to the horizontal clove dimension, shows that the width of 1 deg provides a good compromise between precision of the radiative transfer and total number of cloves. For the retrieval tests presented in the next section we have adopted a constant discretization of the atmosphere with cloves 0.5 km thick and 1 deg wide. This choice will prove to be consistent with the values of spatial resolution assessed, in Sect. 7, for MIPAS2k.

## 6. *Full-2D* retrieval tests on simulated observations

In order to provide an example of the quality of the level 2 products derived from MIPAS2k exploiting the *full-2D* approach, we report results of the retrieval of O<sub>3</sub> VMR carried out on simulated observations. The steps of this retrieval are:

1. A 2D stand-alone forward model generates synthetic spectra for the whole orbit. Simulated observations are obtained by adding to the synthetic spectra a random noise having the r.m.s. deviation of MIPAS2k spectra.
2. The *full-2D* retrieval of O<sub>3</sub> VMR is carried out on the simulated observations. All the geometrical and auxiliary data are the same as at point 1. The initial guess of the O<sub>3</sub> VMR field is derived from the climatological IG2 database [20] (also used for the initial guess in MIPAS operational retrievals); this is a low spatial resolution model defined for six latitudinal bands.
3. The retrieval accuracy is evaluated by comparing the retrieved values with the reference values used to generate the observations simulated at step 1 (the ECMWF O<sub>3</sub> field).
4. The spatial resolution of the retrieval products is evaluated through the perturbation method (described in Sect. 7).

The forward model used at step 1 operates with the same atmospheric discretization as in the *full-2D* of step 2 but calculating the Curtis-Godson integrals (see Sect. 5). In this way the simulated observations do not suffer by the homogeneity assumption within the cloves so that the impact of this assumption is included in the accuracy of the retrieved quantities. At step 2

the only constraint adopted in the retrieval process is the optimal estimation with the initial guess as a-priori information weighted with 200% uncertainty at all altitudes. This weak constraint just prevents matrix singularities due to the lack of target quantity at some altitude.

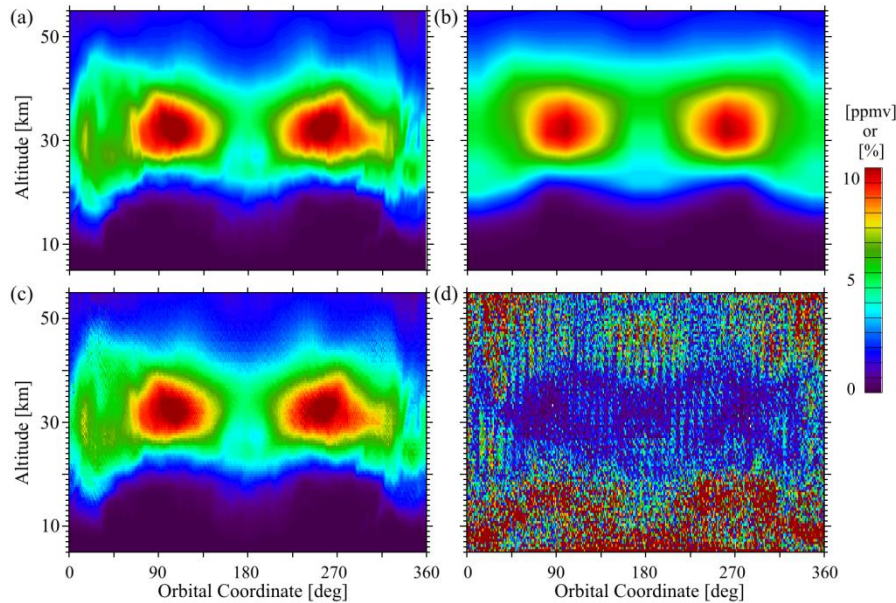


Fig. 6. (a)  $O_3$  VMR distribution used to generate the simulated observations; (b) distribution used as initial guess for the retrieval process; (c) result of the *full-2D* retrieval; (d) relative values of the difference between retrieved and reference  $O_3$  VMRs.

Panels (a) and (b) of Fig. 6 report the reference (ECMWF) and initial-guess (IG2)  $O_3$  fields respectively. These maps are obtained by interpolating the VMR values of the ECMWF and IG2 altitude profiles on all the nodes of the 2D discretization and leaving the plotting program to fill the map with its interpolation criteria. In the *full-2D* the reference and initial guess of each clove is obtained as the average of the values on its four nodes (see panel (a) of Fig. 7). The  $O_3$  field retrieved by the *full-2D* is shown in panel (c) of Fig. 6 while panel (d) of the same figure shows the relative difference between retrieved and reference values. Maps in panels (c) and (d) of Fig. 6 are *full-2D* representations obtained by filling each clove with the color corresponding to its constant value.

Map (d) of Fig. 6 provides an overall picture of the retrieval accuracy. A thorough analysis of these results leads to estimate an accuracy better than 5% in the stratospheric regions where  $O_3$  is mostly present and better than 30% in the UTLS.

A specific example of retrieval performance is provided in Fig. 7 where panel (a) shows, in the *full-2D* representation, a detail of the reference  $O_3$  field (panel (a) of Fig. 6) in correspondence of a fine  $O_3$  structure that is present within the Arctic region. The color scale has been modified, with respect to Fig. 6, to highlight the details of the  $O_3$  structure. We will use this structure to show properties of MIPAS2k that cannot be appreciated in Fig. 6. Panel (b) of Fig. 7 shows the result of the *full-2D* retrieval (this is the enlargement from panel (c) of Fig. 6). The comparison of panels (a) and (b) of Fig. 7 demonstrates how the details of the  $O_3$  structure could be reproduced by MIPAS2k.

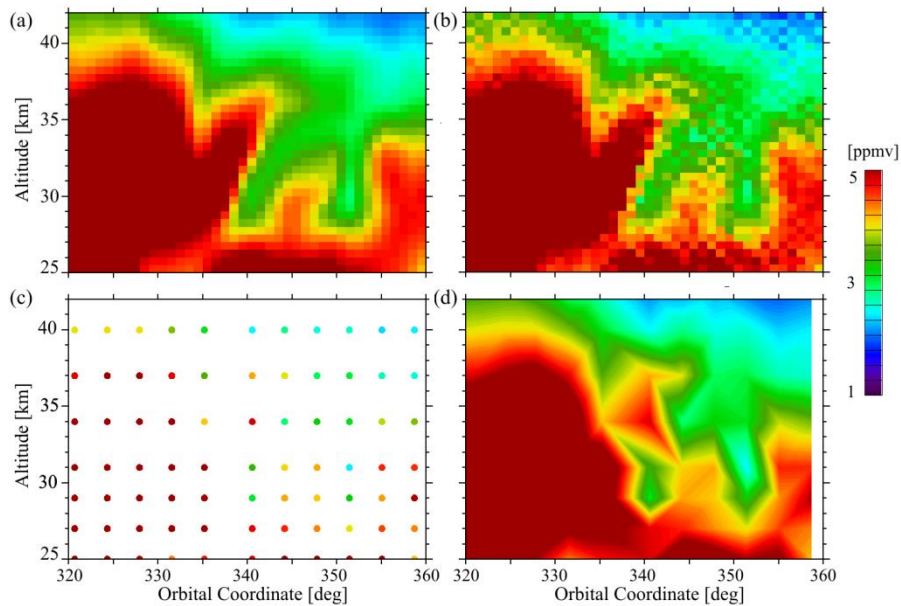


Fig. 7. (a) Detail of the reference O<sub>3</sub> field in *full-2D* representation; (b) result of the *full-2D* retrieval; (c) layout of the retrieval parameters, in the considered atmospheric section, as defined by the Geo-fit; VMR values are represented with the same color scale as in the other panels; (d) O<sub>3</sub> field obtained by interpolating the VMR values of panel (c) over the orbit plane.

In order to compare the performance of MIPAS and MIPAS2k we have exploited the forward model used to generate the MIPAS2k observations to calculate the spectra that would have been generated by MIPAS when observing the same high-resolution atmosphere. For the purpose we have simulated, using the ECMWF fields and the observation geometries of ENVISAT orbit 30958, the standard set of O<sub>3</sub> MWs used for MIPAS retrievals. The Geo-fit analysis system was then employed to retrieve the O<sub>3</sub> profiles along this orbit. Panel (c) of Fig. 7 shows the layout of the retrieval parameters that define, in the geo-fit representation, the VMR distribution (according to the criterion used to generate the MIPAS2D database [13] the horizontal retrieval grid is defined by the mean position of the tangent points of each limb-scan while the vertical grid is defined by the nominal altitudes of the tangent points). In this panel colors are assigned to the grid points to represent the VMR values that, interpolated over the orbit plane by the plotting program, generate the O<sub>3</sub> map reported in panel (d).

A thorough comparison is not possible between the results of MIPAS2k and MIPAS (panels (b) and (d) of Fig. 7 respectively) because of several different strategies adopted in both the instruments and the algorithms (e.g. analyzed MWs, definition of the state vector, graphical representation); however the maps in Fig. 7 clearly show the improvement that can be obtained with MIPAS2k.

## 7. Spatial resolution of MIPAS2k products

The retrieval tests have shown the capability of MIPAS2k to resolve fine atmospheric structures. A quantitative assessment of the spatial resolution would require calculation of the averaging kernel (AK) of the state vector; however the large number of retrieval parameters (see Sect. 8) makes the AK a huge matrix which is difficult to manage. Furthermore, the precision of the AK elements is limited by the building-up of the great number of real-algebra approximations. In order to provide quantitative estimates of the spatial resolution, we have exploited the features of our test to calculate columns of the averaging kernel matrix, for some representative retrieval parameters, using the *perturbation* approach. Actually, we can

directly apply the definition of AK of a parameter (as the derivative of the retrieved value with respect to the true value of the parameter) thanks to the possibility, in a simulated retrieval, to perturb the “true” state vector. In practice we have perturbed the VMR value within a selected clove  $k$  (identified by  $\theta_k$  and  $z_k$  as OC and altitude respectively) of the reference atmosphere in its *full-2D* representation. The difference between VMR fields retrieved from spectra simulated with and without the perturbation in clove  $k$  provides a picture of the 2D AK for the retrieval parameter in this clove. According to [21] we define the vertical resolution of this parameter as the FWHM of the geometric figure subtended by the subset of AK elements that correspond to the value  $\theta_k$  of the OC. In a similar way the horizontal resolution is defined as the FWHM of the geometric figure subtended by the subset of AK elements that correspond to altitude  $z_k$ .

The steps leading to evaluate the spatial resolution are highlighted in Fig. 8. Here panel (a) shows a detail of the reference atmosphere (in the *full-2D* representation) in the Antarctic region; in this map is visible a clove (around 30 km and 180 deg) where the  $O_3$  VMR of the reference atmosphere has been enhanced by 50% on purpose. Panel (b) of Fig. 8 shows the  $O_3$  field retrieved by *full-2D* from the observations simulated with the perturbed reference atmosphere.

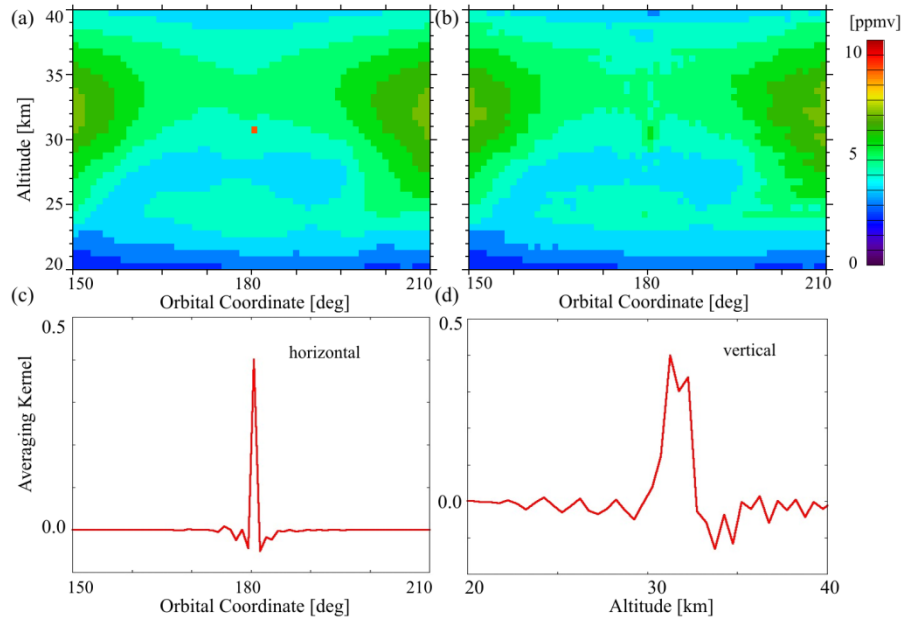


Fig. 8. (a) Detail of the reference atmosphere in the Antarctic region where the  $O_3$  VMR has been enhanced by 50% within a clove around 30 km and 180 deg.; (b)  $O_3$  field retrieved from the observations simulated with the atmosphere in panel (a); (c) and (d) differences, along the OC and altitude of the perturbed clove, between values retrieved with the perturbed and unperturbed clove divided by the perturbation value.

Panels (c) and (d) of Fig. 8 are plots along the OC and altitude of the perturbed clove respectively. They show the difference between values retrieved with the perturbed and unperturbed clove divided by the perturbation value. In order to evaluate the spatial resolutions the geometric figures in panels (c) and (d) are assimilated to triangles whose area is calculated by integrating over the absolute value of the numerical derivatives. The FWHM of the triangle is then calculated by dividing the area by the peak value of the derivative. For this particular test the values calculated for horizontal and vertical resolution are 164 km and 2.5 km respectively. The 50% increment given, in this test, to the VMR in clove  $k$  enables appreciation of differences in the maps of Fig. 8 but may appear a rough approximation for

the numerical calculation of the derivatives representing the AK elements. Actually, several tests were carried out with different increments (1, 10, 50, 100%) on different cloves where  $O_3$  is determined with a precision better than 5%; the results weakly depend on the increment and indicate that, on the average, 200 km is the estimate for horizontal and 2.5 km for vertical resolutions. These numbers show that the clove dimensions, selected for our tests on the basis of only the homogeneity approximation (see Sect. 5), are appropriate for the considered retrieval scenario. We recall here that average values of MIPAS-OR NOM spatial resolutions for  $O_3$  retrieval have been estimated around 3 km the vertical and 300 km the horizontal [22].

## 8. Computational details

The description of the *full-2D* provided in Sect. 5 suggests that the size of the inversion problem could be a drawback of the *full-2D* retrieval approach because of the huge demand of computer resources. In order to provide an estimate, Table 2 shows computational details for the *full-2D* retrieval of  $O_3$  VMR on MIPAS2k observations, and the corresponding figures for the Geo-fit retrieval on real MIPAS observations (both described in Sect. 6) used for the comparison shown in Fig. 7.

**Table 2. Computational Details for the *Full-2D* and the Geo-fit Retrievals**

	MIPAS2k	MIPAS
N <sup>o</sup> of analyzed MWs	2	5
N <sup>o</sup> of spectral points	247016	431347
N <sup>o</sup> of retrieval parameters	54360	2592
N <sup>o</sup> of iterations	6	4
final value of reduced $\chi^2$	1.25	1.03
CPU time*	14h 31m	1h 12m

\*Intel server with two 6-core CPUs X5650.

In a *full-2D* analysis the number of retrieval parameters depends on the number of cloves generated by the 2D discretization of the atmosphere. The value reported in column II of Table 2 for MIPAS2k derives from the choice, adopted in this test, of cloves all equal in size having 0.5 km altitude and 1 latitude deg width. We notice that the size of cloves could be optimized as a function of altitude on the basis of the homogeneity assumption validity (see Sect. 5). A test carried out with *ad hoc* altitude-dependent clove dimensions led to a reduction of the order of 40% in the number of the retrieval parameters that corresponds to roughly reduce the CPU time by a factor of 3. In this test the quality of the retrieval products was not affected by the different clove dimensions.

## 9. Conclusions

The objective of this study was to assess the performance of a satellite limb sounder (MIPAS2k) that, exploiting the heritage of MIPAS, puts forward an evolution of this experiment. With respect to MIPAS the features of MIPAS2k aim at higher geometrical sampling of the atmosphere by exploiting the 1D array detector technology and by degrading the spectral resolution in order to reduce the recording time of each interferogram. These features, as well as other choices operated for MIPAS2k, were taken from the infrared limb sounder (IRLS) proposed as part of the PREMIER experiment. However, MIPAS2k is meant to be less ambitious with respect to IRLS that was designed to operate with 2D array detectors in order to allow for 3D capability in the retrieved atmospheric fields.

We report the performance obtained by MIPAS2k when measuring  $O_3$  fields; this is representative of the results obtained for a wider set of MIPAS main targets that have been considered. For the retrieval of  $O_3$  VMR two MWs were selected among those defined for the IRLS experiment. The IL distribution of each IRLS MW was analyzed in order to achieve the optimal compromise between intensity and altitude coverage with a reasonable number of spectral points. The IL analysis on the observations of two instruments shows that MIPAS2k

W $\Omega$  values surpass by a factor of about 50 the MIPAS values in its nominal observation mode. Furthermore, MIPAS2k observations generate uniform horizontal W $\Omega$  distributions.

On the basis of the IL analysis the trade-off between precision and spatial resolution of the MIPAS2k 2D retrieval products is expected to make the dimension of cloves comparable to the spatial resolutions. Starting from this consideration we propose a new approach to the 2D retrieval strategy (denoted as *full-2D*) in which the retrieval parameter is no longer the element of an altitude profile but the constant value assumed by the atmospheric quantity within a clove of the 2D discretization. Since the *full-2D* strategy can be adopted only if the clove homogeneity is an acceptable assumption, we have compared MIPAS2k spectra calculated for different clove dimensions with and without the clove homogeneity approximation. The result is that the homogeneity assumption generates differences that, in the UTLS, are below the spectral noise level with cloves that are 0.5 km thick and 1 deg wide.

In order to assess the precision of the retrieval products we carried out *full-2D* retrievals on observations simulated with a high resolution model atmosphere. The comparison between the retrieved and the reference O<sub>3</sub> fields indicates a precision better than 5% between 20 and 40 km and better than 30% in the UTLS.

We have shown the ability of MIPAS2k to reconstruct the details of a fine O<sub>3</sub> structure that is present in the adopted high resolution reference atmosphere. We have then compared this performance with the result that would have been produced by MIPAS when measuring the same fine structure. We provided an assessment of the spatial resolution of MIPAS2k products by means of a *perturbation* approach that, thank to the simulated retrieval strategy, can be adopted to evaluate the averaging kernel of the retrieved parameters. In the case of O<sub>3</sub> we have found 200 km and 2.5 km as estimates of the horizontal and vertical resolutions respectively.

The values reported in this paper for MIPAS2k precision and spatial resolutions are not very dissimilar to the numbers reported in the literature for MIPAS. However a thorough comparison of precisions needs to take into account the higher number of observations analyzed by MIPAS that reduce the random error of its products. On the other hand, the spatial resolutions are derived from the averaging kernels and do not take into account the sampling of the atmosphere operated by the retrieval parameters that, in the case of MIPAS2k is much higher in both vertical and horizontal domains.

Finally we remark that the increase of computer resources demanded by a larger set of observations to be analyzed by MIPAS2k (to get a better performance) should not be a concern considering that the digits reported for our test case refer to a relatively plain computing system.

### **Acknowledgments**

The authors acknowledge Anu Dudhia for providing the set of MWs considered in this paper, and Marco Rizzato for contributing to this work within his master thesis. The authors also acknowledge ECMWF for access to data.